Thermochimica Acta, 79 (1984) 91–101
Elsevier Science Publishers B.V., Amsterdam – Printed in The Netherlands

EFFECT OF GRINDING ON THE TEXTURE AND KINETIC STABILITY OF $MnCO_3$, $CdCO_3$ AND $PbCO_3$

J.M. CRIADO and M. GONZÁLEZ

Departamento de Química Inorgánica de la Facultad de Química de la Universidad de Sevilla and Departamento de Investigaciones Físicas y Químicas Centro Coordinado del C.S.I.C., Seville (Spain)

(Received 21 March 1984)

ABSTRACT

The effect of grinding on both the texture and the kinetics of the thermal decomposition of $MnCO_3$, $CdCO_3$ and $PbCO_3$ is studied. The particle size, the crystallite size and the activation energy of the thermal decomposition of these salts is determined as a function of the grinding time. It has been reported, firstly, that the activation energy decreases by increasing the grinding time and, secondly, that the continuous grinding of these materials does not lead to continuous increases of their BET surface but rather causes them to pass through a maximum. Moreover, the higher the lattice energy of these compounds, the lower the effect of grinding on the activation energy of their thermal decomposition and the higher the maximum value reached by the specific area during the grinding. These results have been explained on consideration that the deformation energy stored during the grinding of the $MnCO_3$, $CdCO_3$ and $PbCO_3$ increases with decreasing lattice energy.

INTRODUCTION

The mechanical treatment of materials constitutes an important procedure in chemical technology which is used to enhance the reactivity of solids by increasing their surface area and producing crystal strains. According to Glasson [1], for harder materials these changes are largely due to brittle fracture while softer materials undergo plastic deformation and strain hardening on longer milling. Moreover, it has been reported in the literature [2] that with sufficiently intensive milling it is possible to carry out, at room temperature, solid-state reactions that would otherwise require higher temperatures to take place. A number of reviews [3–7] on the mechanochemistry of inorganic solids have been published recently.

However, it is necessary to point out that most of the above research concerns the study of the influence of grinding on the texture and structure of isolated materials rather than on a series of compounds, when the changes induced by mechanical treatment in both the textural properties and the chemical reactivity can be correlated with the structural properties of the

0040-6031/84/$03.00

solids. The effect of grinding on the texture, structure and kinetic stability of the alkaline-earth carbonates has been studied previously and it was concluded that the grinding of $MgCO_3$, $SrCO_3$ and $BaCO_3$ leads to a decrease in the activation energy of their thermal decomposition which becomes lower as the lattice energy of the salt decreases. These results were interpreted by assuming that the mechanically produced lattice disorder increases with decreasing lattice energy. By contrast, the activation energy of the decomposition of $CaCO_3$ did not undergo significant alterations. This behaviour was attributed [10] to a diminution of the microstrains created during the grinding as a result of the phase transformation calcite → aragonite and aragonite → calcite that were induced in the salt by grinding.

In order to check on the above conclusion it would be interesting to obtain additional information about the effect of the mechanical treatment on the reactivity of other compounds isostructural with the alkaline-earth carbonates. In this paper, the influence of grinding on the texture and kinetic stability of $MnCO_3$, $CdCO_3$ and $PbCO_3$ is studied.

EXPERIMENTAL

An Oliver-Battle planetary ball-mill, model Colerecord 20 A, with a speed of 400 rpm was used. The mill was equipped with a corundum jar (capacity 300 cm^3) containing 10 balls of the same material, 18 mm in diameter. $MnCO_3$, $CdCO_3$ and $PbCO_3$ (Merck r.a.) were used and sample weights of about 4 g ($MnCO_3$ and $CdCO_3$) and 10 g ($PbCO_3$) were ground for periods ranging from 0 to 7 h. The temperature of the sample was monitored during the grinding and it was realized that it was never higher than room-temperature during the mechanical treatment.

The powder X-ray diffraction diagrams of the samples were obtained with a Philips PW 1060 instrument equipped with a scintillation counter, using Cu K_α radiation, a nickel filter and a goniometer scanning rate of $1/8°$ min^{-1}. The slit widths were 1°; 0.2 mm; 1°. The strongest peaks of the samples were chosen for determining the crystallite size. These lines are $2\theta = 31.25°$ for the (104) plane for $MnCO_3$; $2\theta = 30.2°$ for the (104) plane for $CdCO_3$; and $2\theta = 24.7°$ for the (111) plane for $PbCO_3$. These lines were corrected for instrumental broadening by using the profile of the line (101) of the α-quartz that appears at $2\theta = 26.7°$. The crystallite size was calculated using the corrected integral broadening by means of the Scherrer equation [11].

The surface area was measured for the adsorption isotherm of nitrogen (99.99%) at a temperature of 77 K by using the BET method. In order to avoid the influence of the water vapour condensed in the pores, the samples were outgased at 110 °C under a vacuum of 10^{-6} Torr before performing the isotherms. The reproducibility of the specific area was better than 3%. The particle size was determined for the values of the specific surface, by assuming spherical symmetry, from the following equation

$$D_s = \frac{6}{\rho S} 10^4 (\text{Å}) \tag{1}$$

where D_s is the equivalent diameter, expressed in Ångstroms; ρ is the density of the sample; and S is the specific surface.

A Cahn electrobalance (model RG), equipped with a Derivatograph Mark II, that allows the simultaneous recording of both the temperature change and the weight change rate as a function of the temperature (TG and DTG curves, respectively). The TG and DTG curves were recorded under a vacuum of 10^{-4} Torr and a heating rate of 6 K min^{-1}. The starting sample weights used were ~ 23 mg.

The kinetic analyses of DTG and TG data were made using the methods of Sharp and Wentworth [12] and Coats and Redfern [13], that employ, respectively, the following kinetic equations

$$\ln \frac{\mathrm{d}\alpha/\mathrm{d}t}{\mathrm{f}(\alpha)} = \ln A - E/RT \tag{2}$$

and

$$\ln \mathrm{g}(\alpha) - 2 \ln T = \ln \frac{AR}{\beta E} - E/RT \tag{3}$$

where α is the reacted fraction at the temperature T and time t; β is the heating rate; A, the Arrhenius pre-exponential factor; E, the activation energy; R, the gas constant and $\mathrm{f}(\alpha)$ and $\mathrm{g}(\alpha)$ are functions dependent on the reaction mechanism. These two functions are related by the expression

$$\mathrm{g}(\alpha) = \int_0^{\alpha} \mathrm{d}(\alpha)/\mathrm{f}(\alpha) \tag{4}$$

The plot of the left-hand side of eqns. (2) and (3) against the inverse of the temperature leads to a straight line whose slope gives the activation energy. If the proper functions $\mathrm{f}(\alpha)$ and $\mathrm{g}(\alpha)$ have been previously assumed for performing the calculation the two plots would lead to the same values of the activation energy. This fact has previously been used to discriminate for the actual kinetic law [14].

RESULTS

Figure 1 shows the calculated specific surface values for the $MnCO_3$, $CdCO_3$ and $PbCO_3$ samples as a function of the grinding time. It is evident that the surface area does not rise continuously whilst comminution is in progress but reaches a maximum and thereafter decreases with increasing grinding time. The maximum specific surface value reached during grinding

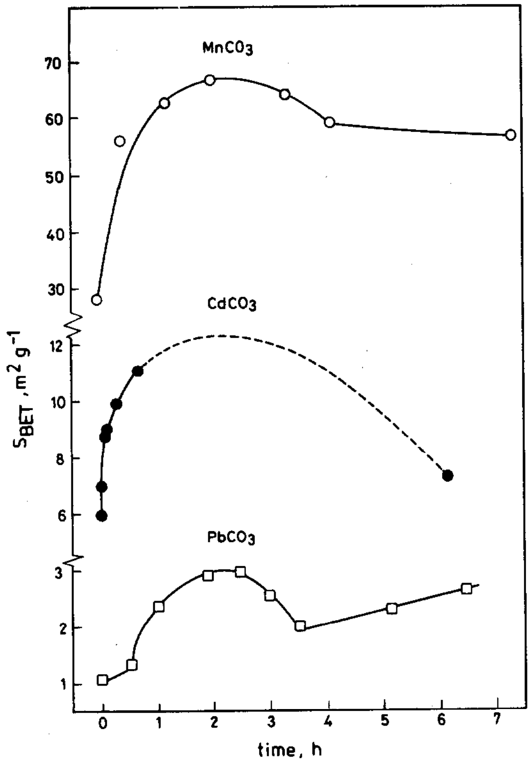

Fig. 1. Specific surface areas of $MnCO_3$, $CdCO_3$ and $PbCO_3$ as a function of the grinding time.

decreases across the series $MnCO_3 > CdCO_3 > PbCO_3$. Almost no influence of the comminution is observed on the specific surface of $PbCO_3$.

The values of the crystallite size of the as-received and the ground samples of the above carbonates determined from the broadening of the X-ray diffraction lines are compared in Tables 1–3 with the particle sizes calculated from the specific surface values of the samples. These data only show a good agreement between both series of parameters in the case of $MnCO_3$.

TABLE 1

Particle size (D_s) and crystallite size (D) of $MnCO_3$ as a function of grinding time

Grinding time (h)	D (Å)	D_s (Å)
0	512	682
0.37	244	328
1.18	205	277
2.00	216	267
3.33	210	277
4.15	210	297
7.37	192	299

TABLE 2

Particle size (D_s) and crystallite size (D) of $CdCO_3$ as a function of grinding time

Grinding time (h)	D (Å)	D_s (Å)
0	588	2098
0.02	551	1774
0.03	496	1498
0.08	453	1383
0.28	397	1272
0.67	314	1138
6.18	223	1801

TABLE 3

Particle size (D_s) and crystallite size (D) of $PbCO_3$ as a function of grinding time

Grinding time (h)	D (Å)	D_s (Å)
0	1054	8737
0.63	383	7291
1.00	342	3805
1.83	365	3326
2.50	311	3338
3.00	350	3516
3.50	297	4695
5.25	343	3987
6.50	343	3596

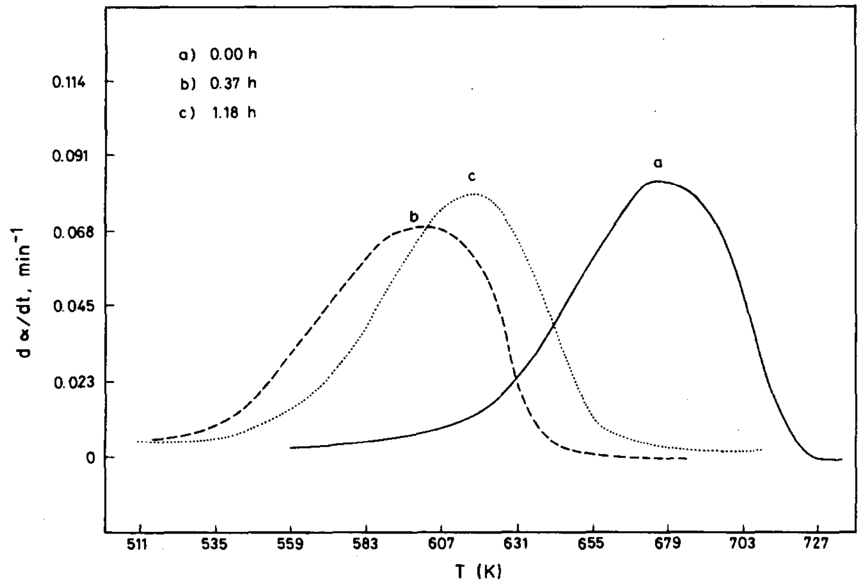

Fig. 2. DTG curves of the thermal decomposition of $MnCO_3$ in vacuum for different grinding times.

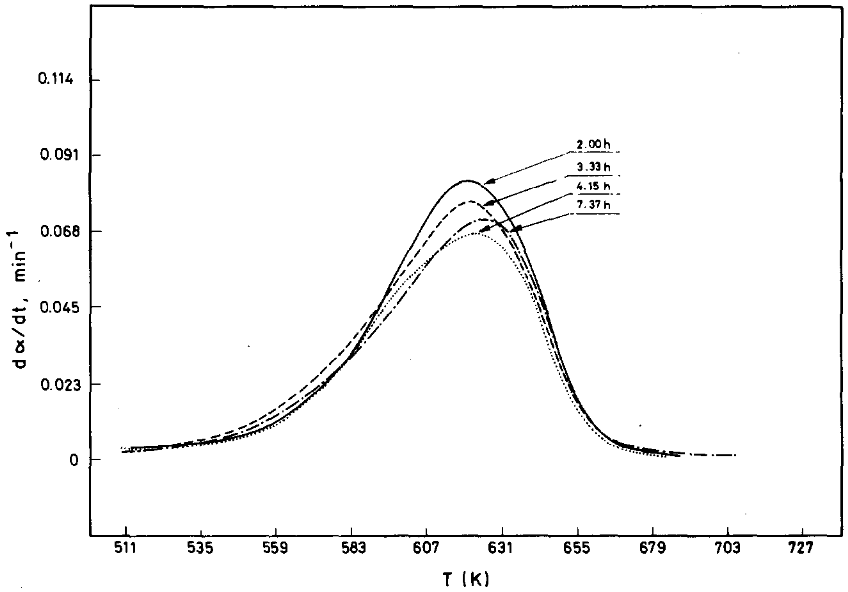

Fig. 3. DTG curves of the thermal decomposition of $MnCO_3$ in vacuum for different grinding times.

The DTG curves of this series of samples ($MnCO_3$, $CdCO_3$ and $PbCO_3$) are included in Figs. 2–8. Both the total change in weight and the X-ray diffraction analyses indicate that the final products of the decomposition of these salts are their corresponding monoxides: MnO, CdO and PbO, respec-

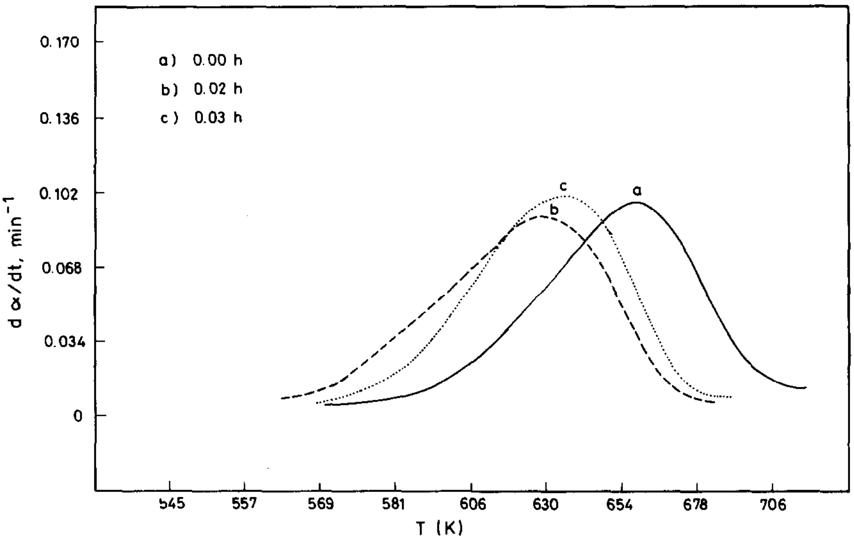

Fig. 4. DTG curves of the thermal decomposition of $CdCO_3$ in vacuum for different grinding times.

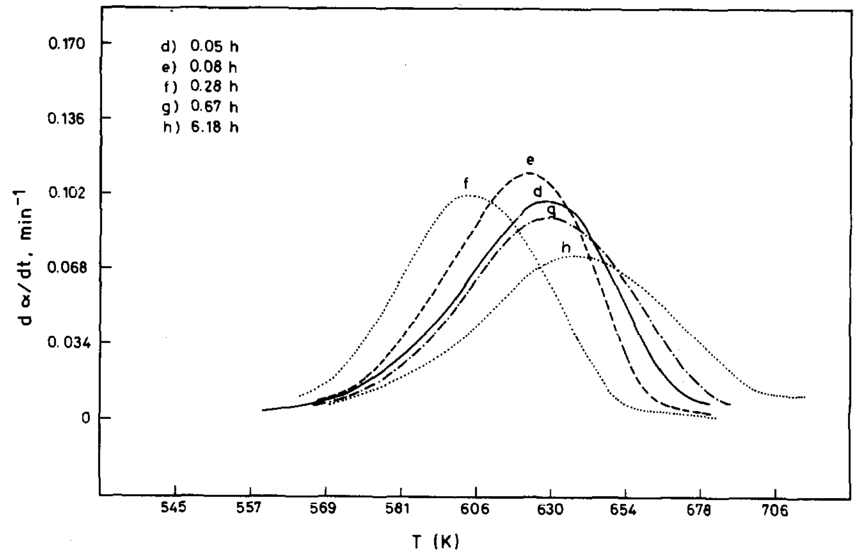

Fig. 5. DTG curves of the thermal decomposition of $CdCO_3$ in vacuum for different grinding times.

tively. Moreover, no decomposition takes place during the grinding, contrary to previous reports [15–17].

The DTG data of $MnCO_3$ and $CdCO_3$ simultaneously fit both eqns. (2) and (3), leading to the same values of the kinetic parameters if a first-order kinetic law (i.e., $f(\alpha) = 1 - \alpha$ and $g(\alpha) = -\ln(1 - \alpha)$) is assumed. The values calculated for the activation energy are plotted vs. the grinding time in Fig. 9.

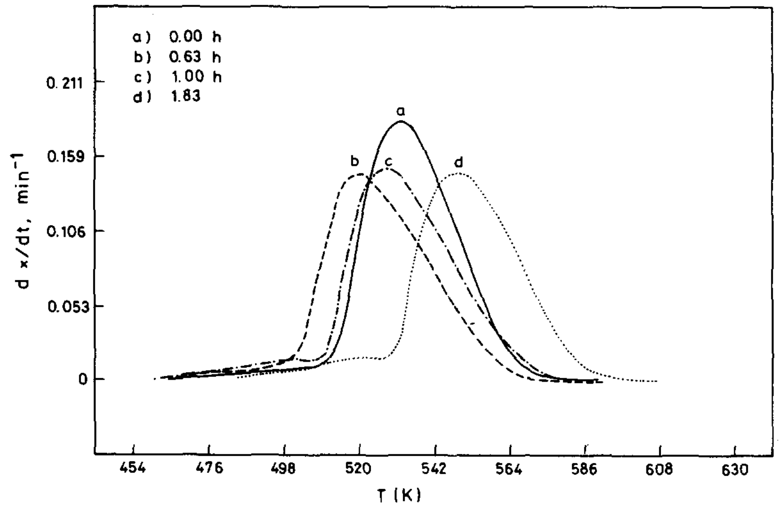

Fig. 6. DTG curves of the thermal decomposition of $PbCO_3$ in vacuum for different grinding times.

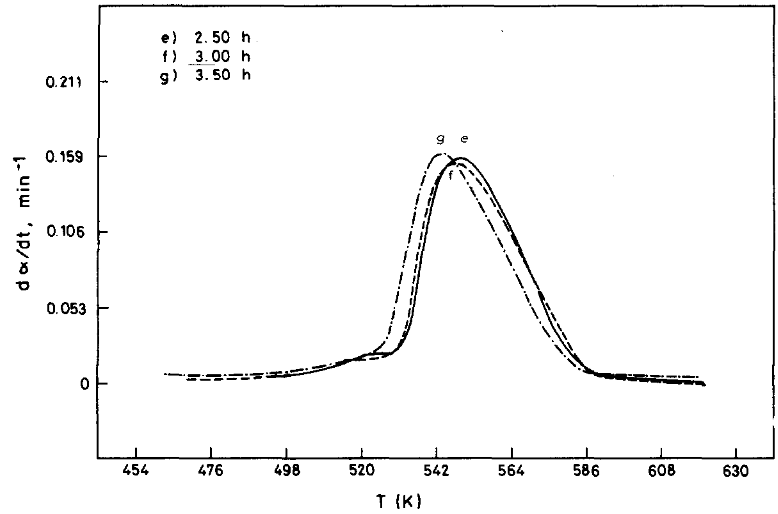

Fig. 7. DTG curves of the thermal decomposition of $PbCO_3$ in vacuum for different grinding times.

On the other hand, the DTG data of the $PbCO_3$ included in Figs. 6–8 do not fit eqns. (1) and (2) simultaneously, regardless of the kinetic law previously assumed for performing the calculation. Thus, the kinetic analysis of these data was not possible. This behaviour can be easily explained taking into account the report [18] that $PbCO_3$ does not decompose according to a single step, like $MnCO_3$ or $CdCO_3$, but decomposes at pressures lower than 1 atm through two consecutive stages that overlap if the thermal decomposi-

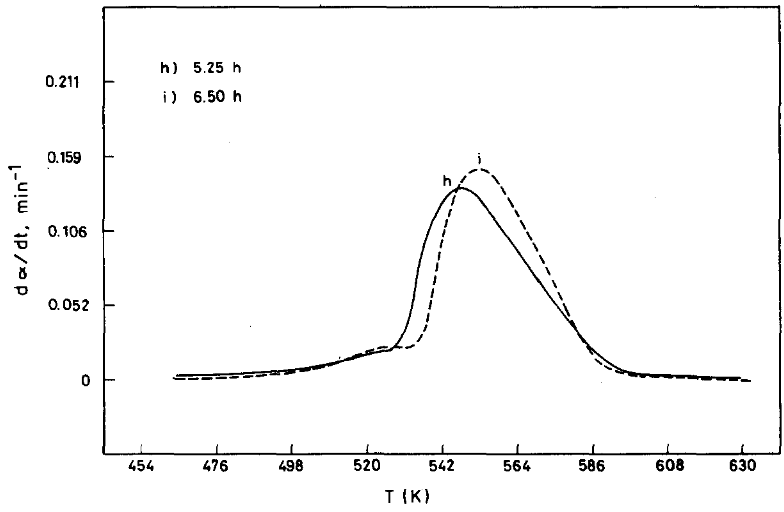

Fig. 8. DTG curves of the thermal decomposition of $PbCO_3$ in vacuum for different grinding times.

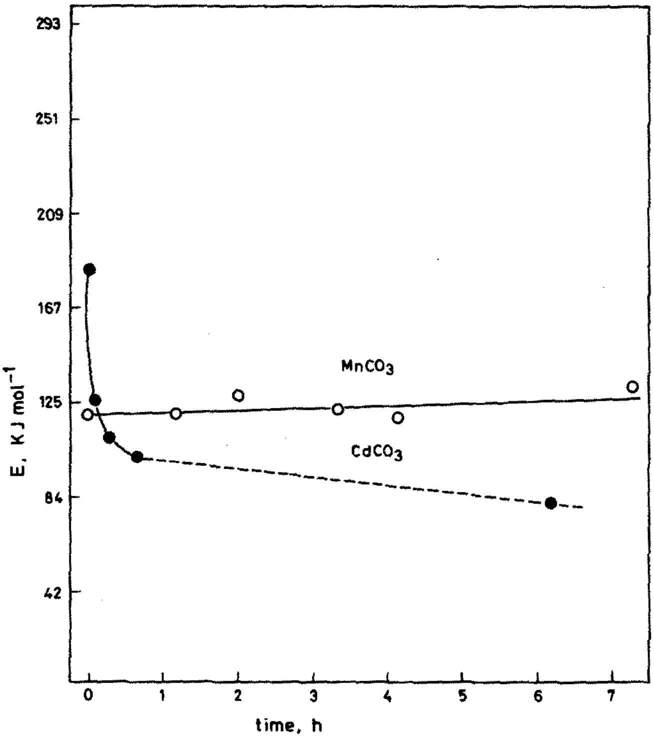

Fig. 9. Activation energy of the thermal decomposition of $MnCO_3$ and $CdCO_3$ as a function of the grinding time.

tion is carried out under vacuum.

$$3\ PbCO_3 \rightarrow PbCO_3 \cdot 2\ PbO + 2\ CO_2$$

$$PbCO_3 \cdot 2\ PbO \rightarrow 3\ PbO + CO_2$$

DISCUSSION

The comparison of both the lattice energies of $MnCO_3$, $CdCO_3$ and $PbCO_3$, included in Table 4, and their specific surface values induced by grinding (Fig. 1) show that the higher the lattice energy the higher the

TABLE 4

Lattice energies for the $MnCO_3$, $CdCO_3$ and $PbCO_3$

Sample	Lattice energy (kJ mol^{-1})
$MnCO_3$	3256
$CdCO_3$	3218
$PbCO_3$	2917

maximum value reached by the specific surface before the cold welding of particles begins. This behaviour can be interpreted, bearing in mind that when the lattice energy increases it would be expected that the slipping of the lattice planes becomes more difficult and, therefore, the fracture of the particles should become easier than the plastic deformation of the crystal. On the other hand, it has been reported in the literature [1,19] that plastic deformation helps form contact between particles and hence, their cold welding. Thus, particle reaggregation would be favoured with regard to the following scheme, explaining the results shown in Fig. 1

lattice energy and particle fracture decrease

$$\mathrm{MnCO_3}\ \ \overset{\longrightarrow}{\underset{\longrightarrow}{\overline{\mathrm{CdCO_3}}}}\ \ \mathrm{PbCO_3}$$

plastic deformation and particle reaggregation increase

The agreement between the values of the particle size of the as-received and ground samples of $MnCO_3$ calculated from both the broadening of the X-ray diffraction patterns and the surface area, respectively (Table 1) seems to show that the crystallite size is the only contribution to the broadening of the X-ray diffraction peaks. However, as far as $CdCO_3$ is concerned, the data in the table indicate that the higher the grinding time, the higher the particle size determined from surface area measurements with regard to the corresponding value calculated from the broadening of the X-ray peaks. This suggests that the influence of microstrains on the X-ray line broadening of $CdCO_3$ is very large. This contribution seems to be still larger in the case of $PbCO_3$ as shown by comparison of the two sets of particle size included in Table 3. Therefore, the conclusion can be reached that the broadening of the X-ray lines of the ground samples of $PbCO_3$ is entirely due to the microstrains induced by the grinding of this compound.

It can be concluded from the above considerations that there is probably an increase of the stored deformation energy induced by the grinding process across the series $MnCO_3 < CdCO_3 < PbCO_3$, which agrees with the interpretation given to the plots of the specific surface values of these samples as a function of the grinding time.

On the other hand, this interpretation also supports the data of the activation energy of the thermal decomposition of $MnCO_3$ and $CdCO_3$ plotted in Fig. 9 vs. grinding time. It is evident that there is no change in the activation energy of the thermal decomposition of $MnCO_3$, which does not seem to undergo plastic deformation during the grinding. However, in the case of $CdCO_3$, whose grinding leads to an enlargement of the microstrain level (i.e., to an increase of the stored deformation energy), a diminution of the activation energy of its thermal decomposition takes place on increasing the grinding time.

In summary, it can be concluded that the deformation energy stored during the grinding of $MnCO_3$, $CdCO_3$ and $PbCO_3$ increases on decreasing lattice energy. Consequently, the higher the lattice energy of these salts, the lower the effect of grinding on the activation energy of their thermal decomposition and the higher the maximum value reached by the specific area during the ball-milling.

REFERENCES

1 D.R. Glasson, Thermochim. Acta, 51 (1981) 45.
2 N. Lefelshtil, S. Nadiv, I.J. Lin and Y. Zimmels, Powder Technol., 20 (1978) 211.
3 I.J. Lin and P. Somasundaran, Powder Technol., 6 (1972) 171.
4 I.J. Lin, S. Nadiv and D.J.M. Grodzian, Miner. Sci. Eng., 7 (1975) 313.
5 P.G. Fox, J. Mater. Sci., 10 (1975) 340.
6 V.V. Boldyrev and E.G. Avvakumov, Russ. Chem. Rev., 40 (1971) 847.
7 I.J. Lin and S. Nadiv, Mater. Sci. Eng., 39 (1979) 193.
8 J.M. Criado, F. Gonzalez and J. Morales, Ceram. Inf., (1978) 715.
9 J.M. Criado, F. Gonzalez and J. Morales, Thermochim. Acta, 32 (1979) 99.
10 J.M. Criado and J.M. Trillo, J. Chem. Soc., Faraday Trans. 1, 71 (1975) 961.
11 P. Scherrer, Göttinger Nachrichter, 2 (1918) 98.
12 J.H. Sharp and S.A. Wentworth, Anal. Chem., 41 (1969) 2060.
13 A.W. Coats and J.P. Redfern, Nature (London), 208 (1964) 68.
14 J.M. Criado, J. Morales and V. Rives, J. Therm. Anal., 14 (1978) 221.
15 J.C. Jamienson and R. Goldsmith, Am. Mineral., 45 (1960) 818.
16 F.P. Bowden, P.G. Fox and J. Soria Ruiz, Nature (London), 220 (1968) 778.
17 D.K. Sigrist, G. Heiniake and U. Steinike, Krist. Tech., 8 (1973) 393.
18 J. Yamaguchi, Y. Sawada, O. Sakurai, K. Uematzu, N. Mizutani and M. Kato, Thermochim. Acta, 35 (1980) 307.
19 F.N. Rhives, Trans. AIME, (1947) 506.